THE ASTROPHYSICAL JOURNAL, 606:L155–L158, 2004 May 10

OGLE 2003-BLG-235/MOA 2003-BLG-53: A PLANETARY MICROLENSING EVENT

I. A. BOND,[1] A. UDALSKI,[2] M. JAROSZYŃSKI,[2,3] N. J. RATTENBURY,[4] B. PACZYŃSKI,[3] I. SOSZYŃSKI,[2] L. WYRZYKOWSKI,[2] M. K. SZYMAŃSKI,[2] M. KUBIAK,[2] O. SZEWCZYK,[2,3] K. ŻEBRUŃ,[2] G. PIETRZYŃSKI,[2,5] F. ABE,[6] D. P. BENNETT,[7] S. EGUCHI,[6] Y. FURUTA,[6] J. B. HEARNSHAW,[8] K. KAMIYA,[6] P. M. KILMARTIN,[8] Y. KURATA,[6] K. MASUDA,[6] Y. MATSUBARA,[6] Y. MURAKI,[6] S. NODA,[9] K. OKAJIMA,[6] T. SAKO,[6] T. SEKIGUCHI,[6] D. J. SULLIVAN,[10] T. SUMI,[3] P. J. TRISTRAM,[4] T. YANAGISAWA,[11] AND P. C. M. YOCK[4]
THE MOA AND OGLE COLLABORATIONS
Received 2004 February 12; accepted 2004 March 10; published 2004 April 15

ABSTRACT

We present observations of the unusual microlensing event OGLE 2003-BLG-235/MOA 2003-BLG-53. In this event, a short-duration (~7 days) low-amplitude deviation in the light curve due to a single-lens profile was observed in both the MOA (Microlensing Observations in Astrophysics) and OGLE (Optical Gravitational Lensing Experiment) survey observations. We find that the observed features of the light curve can only be reproduced using a binary microlensing model with an extreme (planetary) mass ratio of 0.0039^{+11}_{-07} for the lensing system. If the lens system comprises a main-sequence primary, we infer that the secondary is a planet of about 1.5 Jupiter masses with an orbital radius of ~3 AU.

Subject headings: gravitational lensing — planetary systems — stars: individual (MOA 2003-BLG-53, OGLE 2003-BLG-235)

1. INTRODUCTION

Gravitational microlensing occurs when a foreground object passes through or very near the line of sight of a background source star, generating a well-known symmetric light-curve profile. If the foreground lens object is a star with an orbiting planet, then the presence of the planet may be detectable via a brief disturbance in the single-lens light curve (Mao & Paczyński 1991; Gould & Loeb 1992). This effect can potentially be utilized to detect planets with masses ranging from those of gas giants right down to terrestrial planets (Bennett & Rhie 1996).

The short timescales of these deviations, ranging from a few days for giant planets to hours for terrestrial planets, and their unpredictability present considerable challenges in any observational program. While some encouraging results have been obtained (Bennett et al. 1999; Albrow et al. 2000; Rhie et al. 2000; Bond et al. 2002; Jaroszyński & Paczyński 2002), no firm detections of planets by microlensing have been obtained previously.

In this Letter, we report observations, obtained by OGLE (Optical Gravitational Lensing Experiment) and MOA (Microlensing Observations in Astrophysics), of the event OGLE 2003-BLG-235/MOA 2003-BLG-53 (hereafter O235/M53) that was independently detected in both survey programs. We observed a 7 day deviation that was strongly detected in both surveys. We show that an extreme mass ratio binary microlensing model best reproduces the observed features in the light curve.

2. OBSERVATIONS

Presently, Galactic bulge microlensing events are discovered and then reported by the two independently operating survey groups OGLE (Udalski 2003) and MOA (Bond et al. 2001). The microlensing event OGLE 2003-BLG-235 ($\alpha = 18^{h}05^{m}16\overset{s}{.}35$, $\delta = -28°53'42\overset{''}{.}0$, J2000.0) was first identified and reported by the OGLE Early Warning System (Udalski 2003) on 2003 June 22. It was independently detected by MOA on 2003 July 21 and reported as MOA 2003-BLG-53.

OGLE observations were carried out with the 1.3 m Warsaw telescope at Las Campanas Observatory, Chile, which is operated by the Carnegie Institute of Washington, equipped with a mosaic CCD camera with 8192 × 8192 pixels. The images were obtained in the *I* band with an exposure time of 120 s each. The observations presented here come from the OGLE-III phase of the OGLE survey and started in 2001 August. Additional photometry of the star was also collected during the OGLE-II phase (1997–2000). This data set, however, indicates no variability of the object during that period and was not used in further analysis.

MOA observations were carried out from the Mount John Observatory in New Zealand with a 0.6 m telescope equipped with a mosaic CCD camera with 4096 × 6144 pixels. The MOA images were obtained using 180 s exposures with a broadband red filter with its throughput centered on the standard *I* band.

[1] Institute for Astronomy, University of Edinburgh, Blackford Hill, Edinburgh EH9 3HJ, UK; iab@roe.ac.uk.
[2] Warsaw University Observatory, Al. Ujazdowskie 4, PL-00-478 Warsaw, Poland; udalski@astrouw.edu.pl, mj@astrouw.edu.pl, soszynsk@astrouw.edu.pl, wyrzykow@astrouw.edu.pl, msz@astrouw.edu.pl, mk@astrouw.edu.pl, szewczyk@astrouw.edu.pl, zebrun@astrouw.edu.pl, pietrzyn@astrouw.edu.pl.
[3] Department of Astrophysical Sciences, Princeton University, Peyton Hall, Ivy Lane, Princeton NJ 08544-1001; bp@astro.princeton.edu, sumi@astro.princeton.edu.
[4] Department of Physics, University of Auckland, Private Bag 92019, Auckland, New Zealand; nrat001@phy.auckland.ac.nz, p.yock@auckland.ac.nz, paulonieka@hotmail.com.
[5] Universidad de Concepcion, Departmento de Física, Casilla 160-C, Concepcion, Chile.
[6] Solar-Terrestrial Environment Laboratory, Nagoya University, Nagoya 464-8601, Japan; abe@stelab.nagoya-u.ac.jp, sada@stelab.nagoya-u.ac.jp, furuta@stelab.nagoya-u.ac.jp, kkamiya@stelab.nagoya-u.ac.jp, kurata@stelab.nagoya-u.ac.jp, kmasuda@stelab.nagoya-u.ac.jp, ymatsu@stelab.nagoya-u.ac.jp, muraki@stelab.nagoya-u.ac.jp, sako@stelab.nagoya-u.ac.jp, sekiguchi@stelab.nagoya-u.ac.jp.
[7] Department of Physics, University of Notre Dame, 225 Niewland Science Hall, Notre Dame, IN 46556; bennett@emu.phys.nd.edu.
[8] Department of Physics and Astronomy, University of Canterbury, Private Bag 4800, Christchurch, New Zealand; john.hearnshaw@canterbury.ac.nz, pam.kilmartin@canterbury.ac.nz.
[9] National Astronomical Observatory of Japan, Osawa 2-21-1, Mitaka, Tokyo 181-8588, Japan; sachi.t.noda@nao.ac.jp.
[10] School of Chemical and Physical Sciences, Victoria University, P.O. Box 600, Wellington, New Zealand; denis.sullivan@vuw.ac.nz.
[11] National Aerospace Laboratory, Jindaiji 7-44-1, Chofu, Tokyo 182-8522, Japan; tyanagi@nal.go.jp.

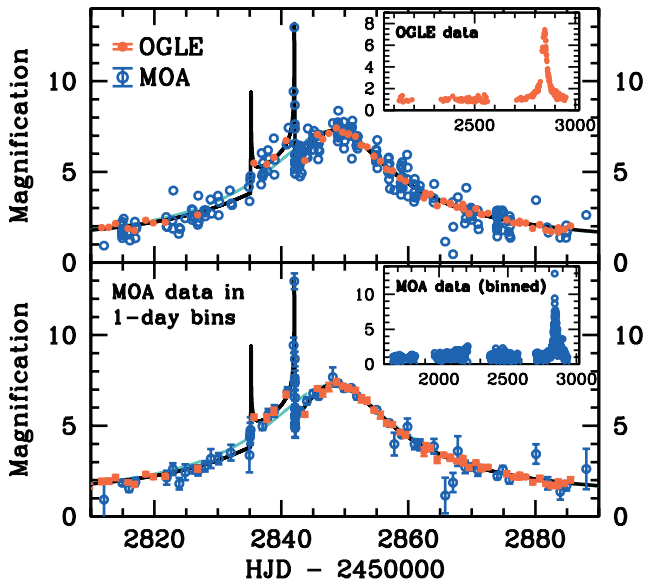

FIG. 1.—Light curve with best-fitting and single-lens models of O235/M53. The OGLE and MOA measurements are shown as red filled circles and open blue circles, respectively. The top panel presents the complete data set during 2003 (*main panel*) and the 2001–2003 OGLE data (*inset*). For clarity, the error bars were not plotted, but the median errors in the OGLE and MOA points are indicated in the legend. The bottom panel is the same as the top panel, but with the MOA data grouped in 1 day bins, except for the caustic crossing nights, and with the inset showing MOA photometry during 2000–2003. The binary- and single-lens fits are plotted in flux units normalized to the unlensed source star brightness of the best planetary fit, and they are indicated by the solid black and cyan dashed curves, respectively.

The photometry was derived using difference imaging analysis carried out independently by the OGLE and MOA teams on their respective data sets. This method is the current state of the art for photometric accuracy in crowded fields (Alard 1999; Alcock et al. 1999). Our analysis resulted in two sets of time-series photometry in the I band corresponding to 183 OGLE measurements and 1092 MOA measurements during 2000–2003.

In Figure 1, we show the light curve for this event on various timescales from 2000 March to the present. The long-term behavior is typical for single point mass microlensing events, and it is similar to the almost 2000 other events discovered in the Galactic bulge since 1993. The unique feature of O235/M53, however, is a short-duration deviation from the profile expected for a single lens, seen clearly in both data sets during 2003 July 14–21. Moreover, a spike, which is characteristic of those binary microlensing events where the source enters or exits a bounded "caustic" region in the magnification map projected on the sky, was observed and well covered by MOA on 2003 July 21. This caustic region was crossed 12% of the overall lens Einstein radius crossing time. This short duration, combined with the small (~25%) amplitude of the photometric deviation in the caustic region interior, suggest an extreme mass ratio binary system.

As well as regular monitoring in the I band, several V-band observations were obtained by OGLE at various magnifications of the event. These were not used in the microlensing modeling, but they were used to constrain the source and lens star properties. By plotting the linearized fluxes in the I and V bands against each other, a model-independent measurement of the color index of the source star was determined. We obtained $V-I = 1.58 \pm 0.02$. Using $E(V-I) = 0.82$ mag for the interstellar reddening toward the source (Sumi 2004), the corrected color index of $(V-I)_0 = 0.76 \pm 0.02$ indicates a G-type source star.

3. LIGHT-CURVE MODELING

The modeling of the observed light curve of O235/M53 was performed independently by three groups using different methods to generate numerical binary microlensing light curves (Bennett & Rhie 1996; Mao & Loeb 2001; Rattenbury et al. 2002), and all three found the solution that is presented in Figure 1. The observable quantities for all microlensing events are the Einstein radius crossing time t_E, the impact parameter u_0 (in Einstein radius units) of the source star trajectory with respect to the lens center of mass, and the time t_0 of the closest approach to the center of mass. For binary microlensing events, one also measures the mass ratio, $q \equiv M_1/M_2$, the transverse separation, a, of the lens components, and the position angle, ϕ, of the binary with respect to the source-lens transverse velocity. For caustic crossing events, one also measures the ratio, $\rho \equiv \theta_*/\theta_E$, of the apparent angular radius of the source star to that of the Einstein ring. In addition to these seven physical parameters, there are two linear scaling parameters between the magnification and the flux units for each passband, giving a total of 11 parameters for the modeling. In our modeling procedure, we searched for local χ^2 minima using minimization procedures that allowed all 11 parameters to vary simultaneously. Our light-curve modeling also employed a surface limb-darkening profile appropriate for a G-type star assuming a metallicity that is approximately solar.

In Table 1, we list the physical microlensing parameters for the best-fitting model shown in Figure 1. This model has $\chi^2 = 1390.49$ for 1267 degrees of freedom (dof) and an extreme mass ratio of $q = 0.0039$, which is a strong indication that the secondary may be a planet. Since microlensing light curves generally allow a much more accurate determination of the mass ratio than the absolute mass of either body, the most sensible way to distinguish planetary microlensing events from those due to binary systems is through a criterion based on the mass ratio parameter q. There is a well-known minimum in the distribution of mass ratios for binary stars and planetary systems, which is known as the "brown dwarf desert." There are few systems known with $0.01 \lesssim q \lesssim 0.1$ (Halbwachs et al. 2000; Chabrier 2003; Mazeh & Zucker 2002). Thus, it is sensible to define the boundary between stellar binary and planetary binary microlensing events in between these q-values to minimize any possible ambiguity. This leads to a criterion of

TABLE 1
MICROLENS MODEL PARAMETERS

Model	M_p/M_*	θ_*/θ_E	a_{proj}/R_E	ϕ (deg)	u_0	t_0	t_E (days)	I_{source} (mag)	χ^2 (1267 dof)	χ^2_{MOA} (1089 dof)	χ^2_{OGLE} (178 dof)
Best-fit	0.0039(+11, −7)	0.00096(11)	1.120(7)	223.8(1.4)	0.133(3)	2848.06(13)	61.5(1.8)	19.70(15)	1390.49	1151.00	239.50
Early caustic	0.0070	0.00104	1.121	218.9	0.140	2847.90	58.5	19.62	1397.87	1149.37	248.49
Best nonplanet	0.0300	0.00088	1.090	187.9	0.144	2846.20	57.5	19.68	1601.44	1229.47	371.98
Single-lens	...	...	...	...	0.222	2847.77	45.2	19.10	2041.45	1624.17	417.28

NOTE.—The units for t_0 are HJD − 2,450,000.

$q < 0.03$ for a planetary microlensing event, and so O235/M53 is clearly in the planetary event category.

We have carried out a systematic search in parameter space to try to find sets of model parameters that might explain the observed light curve with a larger mass ratio. Binary microlensing models with $q \geq 0.1$ that traverse a caustic curve in ~7 days have much larger magnifications inside the caustic curve than is observed for O235/M53. These binary-lens events also have much larger deviations from a single-lens light curve before and after the caustic crossings. As the mass ratio is decreased, the best-fit light curves approach the observed light curves, with much weaker caustic crossing deviations. In Figure 2, we show a close-up of the 7 day deviation with the best-fit planetary model, compared with the best nonplanetary model with $q \geq 0.03$ and best-fit single-lens model. The nonplanetary binary models and single-lens models are strongly disfavored with fit χ^2-values that are larger by $\Delta\chi^2 = 210.96$ and $\Delta\chi^2 = 650.96$, respectively. In both cases, the χ^2 improvement for the best-fit model is quite significant in both the MOA and OGLE data sets (see Table 1). The failure of the nonplanetary binary model can be seen in the Figure 2 insets. This model predicts both stronger caustic signals and significant deviations 13–20 days after the second caustic crossing that are not consistent with the observations. This model also shows some discrepancies at magnifications of less than 2, but these are not as strongly excluded because of the higher photometric uncertainties at lower magnification.

Also shown in Figure 2 is a planetary model with an earlier caustic crossing and a larger planet mass ratio: $q = 0.0070$. This fit represents a distinct local minimum of the χ^2 surface and is disfavored by only $\Delta\chi^2 = 7.37$ or ~2.7 σ. This is not accounted for by our 1 σ uncertainty on $q = 0.0039$. Therefore, we have increased the upper error estimate on the planetary mass ratio to 0.0011, so that the actual uncertainty in q will be bounded by our error estimates at the 3 σ level. In Table 1, we also list the parameters for these alternative models.

Finally, the first OGLE observation after the second caustic crossing indicates a magnification below all of the binary models shown by about 3.6 σ. Such an outlier is not unusual because the real photometric error distributions for crowded field photometry generally have larger wings than a Gaussian distribution. Three of the 183 OGLE measurements are outliers from the best fit by more than 3 σ, and 16 are outliers by more than 2 σ. These outlier points do not appear to cluster in the vicinity of the planetary deviation. If this single data point did indicate a real light-curve deviation, it could be explained by a small variation in the planetary microlensing model, such as a moon orbiting the planet, but there is no nonplanetary model that could help to explain it.

4. FURTHER CONSTRAINTS ON THE SOURCE AND LENS

Most microlensing events have only a single measurable parameter, t_E, that constrains the lens mass, distance, and transverse velocity with respect to the line of sight to the source. However, time-resolved observations of binary event caustic crossings resolve the finite source star effects and partly remove these degeneracies (Alcock et al. 2000; Witt & Mao 1994; Nemiroff & Wickramasinghe 1994; Gould 1994) by allowing a measurement of the Einstein angular radius given by $\theta_E^2 = (4GM_{\rm lens}/c^2)(D_{\rm source} - D_{\rm lens})/(D_{\rm source}D_{\rm lens})$.

Using the flux parameters of the microlensing fit, we obtained $I = 19.70 \pm 0.15$ for the source star and $I = 20.7 \pm 0.4$ for the blended component. This source star magnitude, plus the $V-I$ color from § 2, can be compared with the bulge color-magnitude diagram of Holtzman et al. (1998), and this indicates that the source is probably a bulge star near the main-sequence turnoff. To determine the angular radius of the source star, we used the color-color relations of Bessell & Brett (1988) together with empirical relations between $V-K$ and surface brightness derived from interferometry observations of nearby main-sequence stars (van Belle 1999; di Benedetto 1998).

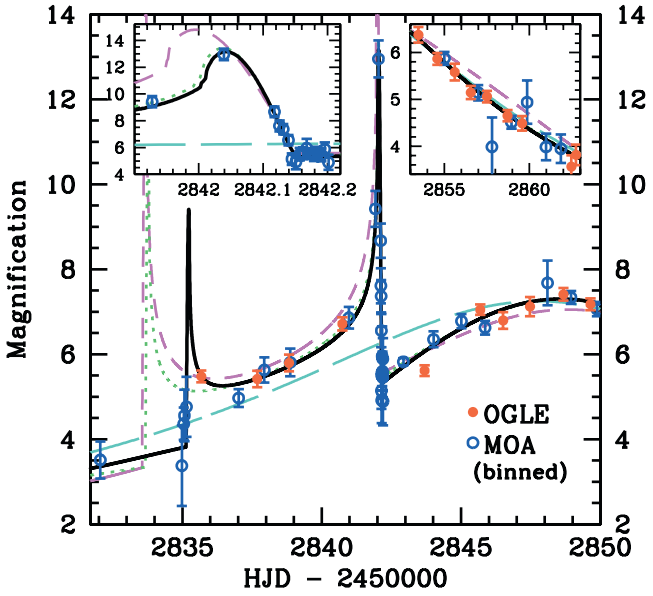

FIG. 2.—Light curve and modeling of O235/M53 during the caustic traverse. The models shown are the best fits for various regimes of the lens system parameter space, normalized as in Fig. 1. These models are the single-lens case (*cyan, long-dashed curve*), the binary lens with $q \geq 0.03$ (*magenta, short-dashed line*), the planetary lens with caustic entry before day 2835 (*green, dotted line*), and the best overall fit with $q = 0.0039$ (*black, solid line*). The insets show the second caustic crossing and a region of the declining part of the light curve where the best-fit nonplanetary binary-lens model fails to fit the data. MOA data on days other than the caustic entry and exit (days 2835 ± 0.5 and 2842 ± 0.5) are placed in 1 day bins.

We find $\theta_* = 0.50 \pm 0.05$ μas, which, combined with our measurement of ρ, yields $\theta_E = 520 \pm 80$ μas. This yields the following relation between the lens mass and distance:

$$\frac{M_{\rm lens}}{M_\odot} = 0.123 \left(\frac{\theta_E}{\rm mas}\right)^2 \frac{D_{\rm source}}{\rm kpc} \frac{x}{1-x}, \quad (1)$$

where $x = D_{\rm lens}/D_{\rm source}$. If we combine this relation with the mass-luminosity relations of Kroupa & Tout (1997) for main-sequence stars, and if we require that the lens luminosity at a given distance does not exceed the blend flux, we obtain an upper limit (with 90% confidence) of $D_{\rm lens} < 5.4$ kpc. Thus, if the lens is a main-sequence star, it must be in the Galactic disk.

In Figure 3, we show equation (1) together with the results of a maximum likelihood analysis based on our measurements of the Einstein ring and its characteristic crossing time. The likelihood function was calculated using the Galactic disk models of Han & Gould (1996). We then obtain (with 90% confidence) $D_{\rm lens} = 5.2^{+0.2}_{-2.9}$ kpc, from which we infer the lensing system to comprise an M2–M7 dwarf star of mass $0.36^{+0.03}_{-0.28}$ $M_\odot$ with a giant planetary companion of $1.5^{+0.1}_{-1.2}$ M_J (Jupiter masses). The planet is in a wide orbit with a transverse separation of $3.0^{+0.1}_{-1.7}$ AU.

Another possibility for the lens is that it could be a remnant object such as a white dwarf, neutron star, or black hole. If the

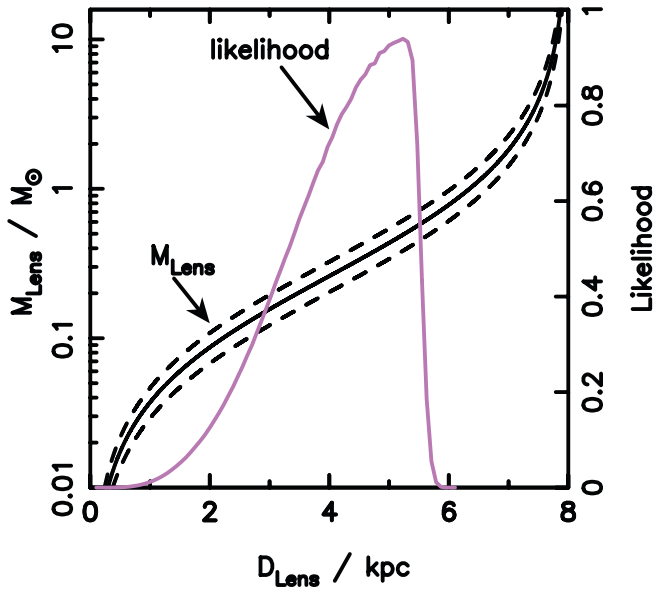

FIG. 3.—Constraints on the distance to O235/M53 and its mass. Our measurement of the angular size of the Einstein ring constrains the lens mass and distance to lie on the solid curve. The curve is bounded above and below by the black dashed curves because of the uncertainty in this measurement. The likelihood function (shown by the magenta curve) is for a main-sequence disk star prior to the lens star, with the sharp cutoff being due to the constraints imposed by the measured lens flux.

lens is a white dwarf with mass 0.6 $M_\odot$, equation (1) would place it at a distance of 5.5 kpc. In this case, the microlensing parameters would imply a 2.5M_J planet orbiting the white dwarf with a transverse separation of 2.8 AU.

5. DISCUSSION

In § 3, we concluded that the observed light curve of O235/M53 is best described by a binary lensing model with an planetary mass ratio of $q = 0.0039$. Our definition of the planetary nature of the secondary lens by means of the mass ratio is optimal when the mass ratio can be measured, but it is useful to consider other possible definitions. Another potential dividing line between planets and brown dwarfs is the solar metallicity threshold for sustained deuterium burning at 13.6M_J, although deuterium burning itself has little relevance for planet formation.

The situation in the case of O235/M53 was helped by the measurement of finite source effects. If the lens is a main-sequence star, then, as shown in the previous section, it must be an M dwarf with an ~1.5M_J planetary companion.[12] There is a nonnegligible chance that the lens is a white dwarf, and a much smaller chance that it is a neutron star, but in both cases, a planetary companion below the nominal 13.6M_J threshold is required. Only in the unlikely case of a massive black hole primary could the secondary be outside the range traditionally associated with a planet.

There are some prospects for follow-up observations of this event. Our measurements of the finite source effects imply a proper motion of the lens with respect to the source of $\mu = \theta_E/t_E = 3.1 \pm 0.4$ mas yr^{-1}. High-resolution imaging carried out ~10 years from now with the *James Webb Space T elescope* or with adaptive optics systems should be able to resolve the lens and source stars, providing direct measurements (Han & Chang 2003; Alcock et al. 2001) of the color and brightness of the lens as well as confirmation of the proper-motion measurement.

We present these observations as a demonstration of the planetary microlensing phenomenon. The power of microlensing is in its ability to acquire statistics on many systems (Bennett & Rhie 2002). These include planets in wide orbits, very low mass planets, and even planets in other galaxies (Covone et al. 2000; Bond et al. 2002). The challenge now for the microlensing community is to develop effective strategies for finding more planetary microlensing events.[13]

The MOA project is supported by the Marsden Fund of New Zealand, the Ministry of Education, Culture, Sports, Science, and Technology (MEXT) of Japan, and the Japan Society for the Promotion of Science (JSPS). Partial support to the OGLE project was provided by the following grants: the Polish State Committee for Scientific Research grant 2P03D02124 to A. Udalski and grant 2P03D01624 to M. Jaroszyński, and the NSF grant AST 02-04908 and NASA grant NAG5-12212 to B. Paczyński. A. Udalski, I. Soszyński, and K. Żebruń also acknowledge support from the grant "Subsydium Profesorskie" of the Foundation for Polish Science. Support was also provided by grants AST 02-06187 (NSF) and NAG5-13042 (NASA) to D. P. Bennett.

[12] The only other M dwarf star known to have planetary companions is Gliese 876 (Marcy et al. 2001).

[13] Numerical photometry of OGLE 2003-BLG-235/MOA 2003-BLG-53 is available from the Web sites for OGLE http://ogle.astrouw.edu.pl and MOA http://www.physics.auckland.ac.nz/moa.

REFERENCES

Alard, C. 1999, A&A, 343, 10
Albrow, M. D., et al. 2000, ApJ, 534, 894
Alcock, C., et al. 1999, ApJ, 521, 602
———. 2000, ApJ, 541, 270
———. 2001, Nature, 414, 617
Bennett, D. P., & Rhie, S. H. 1996, ApJ, 472, 660
———. 2002, ApJ, 574, 985
Bennett, D. P., et al. 1999, Nature, 402, 57
Bond, I. A., et al. 2001, MNRAS, 327, 868
———. 2002, MNRAS, 333, 71
Bessell, M. S., & Brett, J. M. 1988, PASP, 100, 1134
Chabrier, G. 2003, ApJ, 586, L133
Covone, G., de Ritis, R., Dominik, M., & Marino, A. A. 2000, A&A, 357, 816
di Benedetto, G. P. 1998, A&A, 339, 858
Gould, A. 1994, ApJ, 421, L71
Gould, A., & Loeb, A. 1992, ApJ, 396, 104
Halbwachs, J. L., Arenou, F., Mayor, M., Udry, S., & Queloz, D. 2000, A&A, 355, 581
Han, C., & Chang, H. Y. 2003, MNRAS, 338, 637
Han, C., & Gould, A. 1996, ApJ, 467, 540
Holtzman, J. A., et al. 1998, AJ, 115, 1946
Jaroszyński, M., & Paczyński, B. 2002, Acta Astron., 52, 361
Kroupa, P., & Tout, C. A. 1997, MNRAS, 287, 402
Mao, S., & Loeb, A. 2001, ApJ, 547, L97
Mao, S., & Paczyński, B. 1991, ApJ, 374, L37
Marcy, G.W., et al. 2001, ApJ, 556, 296
Mazeh, T., & Zucker, S. 2002, Rev. Mod. Astron., 15, 133
Nemiroff, R. J., & Wickramasinghe, W. A. D. T. 1994, ApJ, 424, L21
Rattenbury, N. J., Bond, I. A., Skuljan, J., & Yock, P. C. M. 2002, MNRAS, 335, 159
Rhie, S. H., et al. 2000, ApJ, 533, 378
Sumi, T. 2004, MNRAS, 349, 193
Udalski, A. 2003, Acta Astron., 53, 291
van Belle, G. T. 1999, PASP, 111, 1515
Witt, H., & Mao, S. 1994, ApJ, 430, 505